



CHORUS

This is the accepted manuscript made available via CHORUS. The article has been published as:

Robust 2-Qubit Gates in a Linear Ion Crystal Using a Frequency-Modulated Driving Force

Pak Hong Leung, Kevin A. Landsman, Caroline Figgatt, Norbert M. Linke, Christopher Monroe, and Kenneth R. Brown

Phys. Rev. Lett. **120**, 020501 — Published 9 January 2018

DOI: [10.1103/PhysRevLett.120.020501](https://doi.org/10.1103/PhysRevLett.120.020501)

Robust two-qubit gates in a linear ion crystal using a frequency-modulated driving force

Pak Hong Leung,^{1,*} Kevin A. Landsman,² Caroline Figgatt,²
 Norbert M. Linke,² Christopher Monroe,² and Kenneth R. Brown^{1,3}

¹*School of Physics, Georgia Institute of Technology, Atlanta, Georgia 30332, USA*

²*Joint Quantum Institute and Joint Center for Quantum Information and Computer Science,
 University of Maryland, College Park, MD 20742, USA*

³*Schools of Chemistry and Biochemistry and Computational Science and Engineering,
 Georgia Institute of Technology, Atlanta, Georgia 30332, USA*

(Dated: November 29, 2017)

In an ion trap quantum computer, collective motional modes are used to entangle two or more qubits in order to execute multi-qubit logical gates. Any residual entanglement between the internal and motional states of the ions results in loss of fidelity, especially when there are many spectator ions in the crystal. We propose using a frequency-modulated (FM) driving force to minimize such errors. In simulation, we obtained an optimized FM two-qubit gate that can suppress errors to less than 0.01% and is robust against frequency drifts over ± 1 kHz. Experimentally, we have obtained a two-qubit gate fidelity of 98.3(4)%, a state-of-the-art result for two-qubit gates with 5 ions.

Ion traps are a leading candidate for the realization of a quantum computer. Magnetically insensitive qubit energy splittings, long coherence times, and high-fidelity state initialization and detection [1, 2] prove to be significant advantages for trapped ion qubits. Individual qubit addressing and single-qubit gates with error rates on the order of 10^{-5} per gate have been achieved [1, 3–5]. Multiple qubits can be entangled through state-dependent forces driven by external fields [6–9], and for exactly two ions, entangling gate fidelities routinely exceed 99% and in some cases 99.9%. [10–15].

With increasing ion number, however, the motional modes bunch in frequency, which means exciting only a single motional mode becomes prohibitively slow. Alternatively, the state-dependent driving forces can couple to all modes of motion. A number of schemes have been proposed for disentangling the internal qubit states from the motional states of all modes by introducing variations to the driving force during the gate. One way to achieve this goal is amplitude modulation (AM) of the driving field [16, 17]. Several experiments have adopted this method and have achieved a 2 to 5% error [18–20]. Discrete phase modulation (PM) has also been proposed for the same purpose, but the number of pulses in the sequence increases exponentially with the number of ions [21]. Moreover, discrete changes in laser amplitude and phase are hard to implement physically, especially when we perform fast gates.

We propose a novel decoupling method through continuous frequency modulation (FM), theoretically equivalent to continuous PM, which involves only small and smooth oscillations of the detuning of the applied field. First, we explain the coherent displacement of the ion

chain’s motional modes during the Mølmer-Sørensen (MS) gate. Then, we describe how the residual displacement of the ions can be minimized in a way which is robust to small changes in trap frequency. Next, we experimentally demonstrate this gate in a chain of 5 $^{171}\text{Yb}^+$ ions. Finally, we discuss extensions of the method to larger ion chains, with 17 ions as an example.

To entangle two qubits with the MS gate, we apply a state-dependent driving force near the sideband frequencies. As a result, each motional mode experiences a coherent displacement characterized by the operator [16, 17]:

$$\hat{D}(\hat{\alpha}_k) = \exp\left(\hat{\alpha}_k a_k^\dagger - \hat{\alpha}_k^\dagger a_k\right),$$

$$\hat{\alpha}_k(t) = \frac{\Omega}{2}(\eta_{i,k}\sigma_\phi^i + \eta_{j,k}\sigma_\phi^j) \int_0^t e^{i\theta_k(t')} dt' \quad (1)$$

where Ω is the carrier coupling strength, $\eta_{i,k}$ and $\eta_{j,k}$ are the Lamb-Dicke parameters of ions i and j with respect to mode k , σ_ϕ^i and σ_ϕ^j are bit-flip Pauli operators for the addressed ions, and $\theta_k(t) = \int_0^t \delta_k(t') dt'$ and $\delta_k(t)$ are the phase and detuning of the driving force relative to mode k . If the qubits are at the $+1$ eigenstate of both σ_ϕ^i and σ_ϕ^j , the displacement is:

$$\alpha_k(t) = \frac{\Omega}{2}(\eta_{i,k} + \eta_{j,k}) \int_0^t e^{i\theta_k(t')} dt' \quad (2)$$

We may visualize the trajectory of $\alpha_k(t)$ over time by plotting it in the complex plane. This is the phase space trajectory (PST) of the motional mode k . For a total gate time τ , $\alpha_k(0) = 0$ and $\alpha_k(\tau)$ are the beginning and end points of the PST.

Due to the state-dependent nature of $\hat{\alpha}_k(t)$, different eigenstates of σ_ϕ^i and σ_ϕ^j follow different PSTs. If any of

* pleung6@gatech.edu

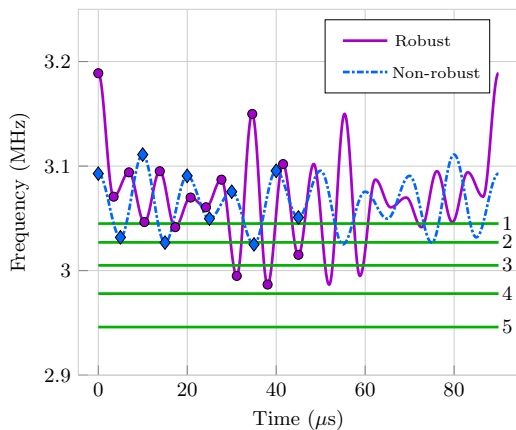


FIG. 1. Robust (violet, solid) and non-robust (blue, dash-dotted) FM pulses for 2-qubit gate optimized for 5 ions, both with a gate time of $90 \mu\text{s}$. Green lines are experimental sideband frequencies, labeled 1 to 5, the first one being the common mode frequency. The pulses are designed to be symmetric in time. The dots and diamonds are the vertices of the frequency and represent the control parameters allowed to vary in our optimization algorithm.

the $\alpha_k(\tau)$ is non-zero, there is residual entanglement between the internal and motional state spaces, which leads to a mixed internal state. This lowers the overall gate fidelity ($F = |\langle \psi_{final} | \psi_{ideal} \rangle|^2$). Given that $|\alpha_k| \ll 1$, we find that the consequent gate error may be estimated as:

$$\varepsilon \equiv 1 - F \approx \sum_{k=1}^N |\alpha_k(\tau)|^2 \quad (3)$$

Minimizing $|\alpha_k|$ is therefore the most straightforward criterion for an optimized gate. However, the gate is sensitive to small drifts in sideband frequencies ($\delta_k \rightarrow \delta_k + \delta_1$ and $\delta_1 \ll 1/\tau$), an imperfection which we often observe in experiments. The frequency dependence of $\alpha_k(\tau)$ can be canceled to the first order by setting the time-averaged position of $\alpha_k(t)$ to zero.

$$\alpha_{k,avg} \propto \int_0^\tau \int_0^t e^{i\theta_k(t')} dt' dt = 0 \quad (4)$$

It turns out that if we only consider symmetric pulses ($\delta_k(\tau - t) = \delta_k(t)$), minimizing $\alpha_{k,avg}$ also minimizes $\alpha_k(\tau)$.

In our scheme, we modulate the driving frequency during the gate to minimize the gate error. The trajectory $\alpha_k(t)$ moves with constant speed but varying angular rate $\delta_k(t)$. Therefore, FM allows us to control the curvature and thus the shapes and end points of the PSTs. We let the frequency assume a symmetric, oscillatory pattern (see example in Fig. 1). The vertices (local maxima and minima) of the oscillations are set to be evenly spaced in

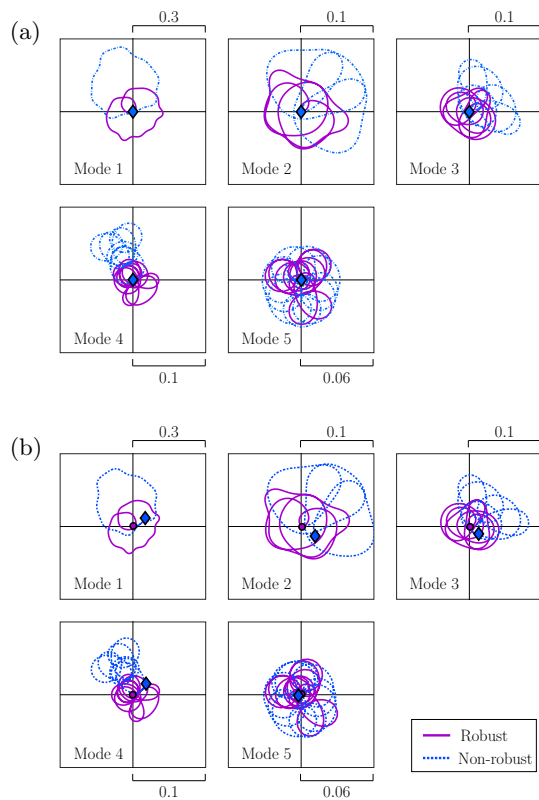


FIG. 2. Simulated PSTs with: (a) no frequency error and (b) -1 kHz sideband drift, using the FM pulses shown in Fig. 1. The end points for the robust pulse (circles) return to the starting point with the drift, whereas those for non-robust (diamonds) fail to do so. The horizontal and vertical axes represent the quadratures $x_k \sim a_k^\dagger + a_k$ and $p_k \sim i(a_k^\dagger - a_k)$ respectively.

time and are the only variable control parameters in our optimization. The vertices are connected with sinusoidal functions, which leads to a smooth and continuous frequency profile. The function to be minimized is $|\alpha_{k,avg}|^2$ for robust pulses and $|\alpha_k|^2$ for non-robust. The number of vertices used is increased until we successfully converge to a solution with errors much lower than 0.01%. Detailed derivations for equations (3) and (4) as well as the optimization process are provided in the Supplemental Material.

Both robust and non-robust versions of the gate are tested on our 5-ion quantum computer. In our setup, 5 $^{171}\text{Yb}^+$ ions are held in an rf Paul trap with a radial trap frequency of 3.045 MHz and an average ion separation of about $5 \mu\text{m}$. Our qubit is defined by the ground hyperfine states $^2\text{S}_{1/2}, |F=0\rangle$ and $^2\text{S}_{1/2}, |F=1\rangle$ with an energy splitting of $2\pi \times 12.642821 \text{ GHz}$ [1]. Initially, all ions are cooled to close to the motional ground state (≈ 0.1 phonons) and then optically pumped to the $|0\rangle$ state. Quantum gates are implemented using a beatnote generated by counter-propagating Raman laser beams that are capable of addressing any individual qubit [18].

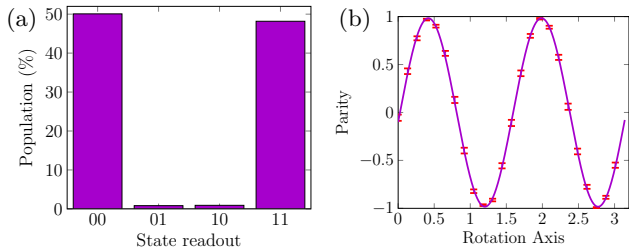


FIG. 3. (a) State population and (b) parity scan of the two qubits after the optimized and robust two-qubit gate shown in Fig. 1, indicating a fidelity of 98.3(4)%.

The 5 transverse motional sidebands are experimentally determined and used to find the optimal FM pulses for the 2-qubit gate. We increase the number of oscillations (degrees of freedom) for optimization until we find a pulse with low errors. With a fixed gate time of 90 μ s, the optimized robust pulse consists of 13 oscillations, whereas the non-robust version has only 9 (Fig. 1). The driving frequency crosses the sidebands multiple times, which contrasts with other implementations of MS gates that avoid sideband resonance.

PSTs are plotted for no frequency error and for a 1 kHz frequency drift for both robust and non-robust pulses in Fig. 2. With the drift, the end points of the robust trajectory (circles) stick to the origin, whereas those of the non-robust (diamonds) deviate from the starting point, causing an estimated error of about 0.5%. This proves the importance of the robustness criterion.

We present the results on entangling two neighboring ions on one edge of the ion chain in the robust case. The output population and parity are measured and shown in Figs. 3(a) and (b), giving a SPAM-corrected fidelity of 98.3(4)%. This is among the highest fidelities achieved for multi-qubit gates in the presence of spectator ions [18]. Using the robust gate, we also successfully perform a CNOT gate with 98.6(7)% fidelity and generate a 3-qubit GHZ state with 92.6(3)% fidelity. The 1% error level observed is partially attributed to laser intensity fluctuations ($\sim 2\%$), which breaks the assumption of constant laser power during the gate.

In order to lower the overall laser intensity Ω , each 90 μ s pulse is performed twice for each gate, with a combined gate time of 180 μ s. The Ω required is $2\pi \times 600$ kHz in carrier Rabi frequency, which is much larger than $2\pi \times 151$ kHz as expected by simulation. The discrepancy is most likely due to an overestimate of the Lamb-Dicke parameters in our simulation. The high power used worsens other error sources such as Raman scattering, off-resonant excitation, and crosstalk with other qubits [11, 12].

The theoretically estimated gate error is plotted as a

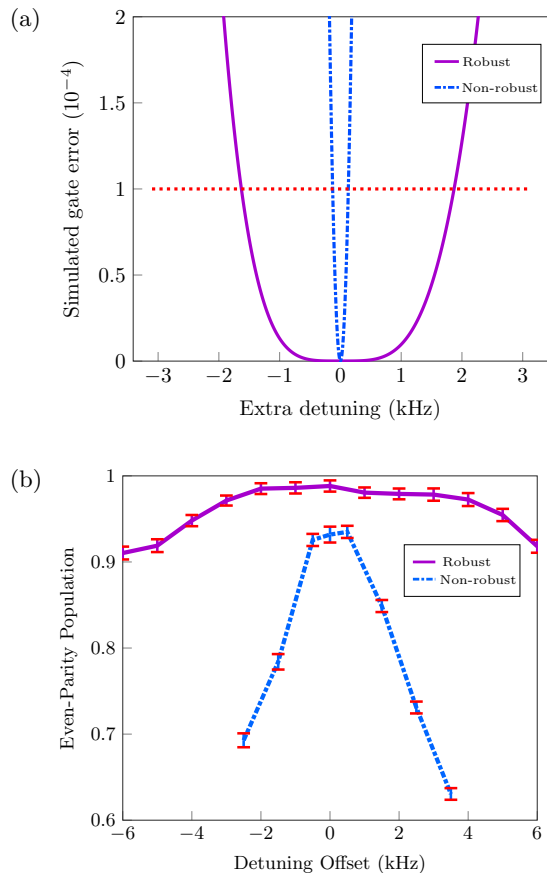


FIG. 4. (a) Simulated gate error and (b) Experimental even-parity populations of the two qubits after the gate for a range of detuning offsets. The robust gate has a significantly better performance than non-robust in both theory and experiment

function of frequency drift in Fig. 4(a) to compare the robust pulse with non-robust. A typical error threshold for high-fidelity gates is 0.01%. The robust pulse can tolerate frequency errors up to ± 1.5 kHz, whereas the non-robust less than ± 0.1 kHz. The non-robust pulse has a quadratic dependence on the drift, whereas the robust version has a quartic dependence. This is expected, since error is proportional to displacement squared, and the first-order dependence of the displacement on drift is canceled out in the robust case.

To determine the impact of sideband drifts, we experimentally run the two gates over a range of symmetric detuning offsets (Fig. 4(b)). The robust version has even-parity population higher than 90% for frequency offsets up to ± 5 kHz, whereas the non-robust gate has significantly lower fidelity and tolerance towards frequency errors (within ± 1 kHz), confirming that the robust method improves fidelity significantly by canceling errors due to frequency drifts.

To test the scalability of our method, we run a similar optimization for 17 ions, motivated by the 17-qubit surface code proposed for quantum error correction [22–25].

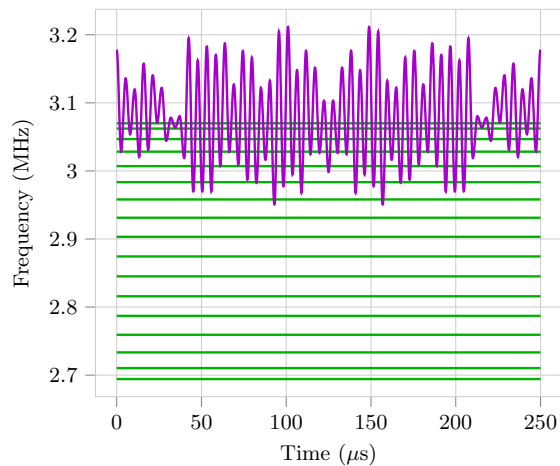


FIG. 5. Optimized FM two-qubit gate for 17 ions. The sideband frequencies (green) are obtained by simulations

The sideband frequencies are calculated from a simulated anharmonic ion trap with an average ion separation of about $3.5 \mu\text{m}$. Such high ion density may be challenging to realize with current technology, but that does not pose a fundamental physical limit to experiments.

The robust FM pulse obtained consists of 47 oscillations within a gate time of $250 \mu\text{s}$ (Fig. 5). The gate can tolerate a frequency drift of 500 Hz for an error threshold of 0.01%. Apparently, the gate is more sensitive to frequency errors due to an increased number of motional modes and a longer gate time.

The power required (Ω) for the two-qubit gate ranges from $2\pi \times 115 \text{ kHz}$ for neighboring ions to $2\pi \times 249 \text{ kHz}$ for the furthest separated ions ($\approx 1:2$ ratio between lowest and highest). This is an encouraging result. Previous simulation results indicate that two-qubit gate time and power increase very quickly with the distance between the ions. But by using a flexible and well-designed optimization program, we have found an FM pulse that can overcome this difficulty.

We have shown that we can perform high-fidelity two-qubit gates in a 5-ion trap using frequency modulation. In theory, the optimized robust FM pulse can suppress errors in gate fidelities to below 0.01% for up to a $\pm 1.5 \text{ kHz}$ frequency offset for 5 $^{171}\text{Yb}^+$ ions. The gate is used to maximally entangle two ions in experiment and has a fidelity of 98.3(4)%. We speculate that in the near future, we will attain over 99.9% fidelity previously achieved with 2-ion chains [10–12].

We would like to thank Todd Green, Luming Duan, and Gang Shu for useful discussions. This work was supported by the Office of the Director of National Intelligence - Intelligence Advanced Research Projects Activity through ARO contract W911NF-10-1-0231 and the ARO MURI on Modular Quantum Systems.

- [1] S. Olmschenk, K. C. Younge, D. L. Moehring, D. N. Matsukevich, P. Maunz, and C. Monroe, *Phys. Rev. A* **76**, 052314 (2007).
- [2] R. Noek, G. Vrijsen, D. Gaultney, E. Mount, T. Kim, P. Maunz, and J. Kim, *Opt. Lett.* **38**, 4735 (2013).
- [3] K. R. Brown, A. C. Wilson, Y. Colombe, C. Ospelkaus, A. M. Meier, E. Knill, D. Leibfried, and D. J. Wineland, *Phys. Rev. A* **84**, 030303 (2011).
- [4] T. P. Harty, D. T. C. Allcock, C. J. Ballance, L. Guidoni, H. A. Janacek, N. M. Linke, D. N. Stacey, and D. M. Lucas, *Phys. Rev. Lett.* **113**, 220501 (2014).
- [5] D. P. L. Aude Craik, N. M. Linke, M. A. Sepiol, T. P. Harty, J. F. Goodwin, C. J. Ballance, D. N. Stacey, A. M. Steane, D. M. Lucas, and D. T. C. Allcock, *Phys. Rev. A* **95**, 022337 (2017).
- [6] K. Mølmer and A. Sørensen, *Phys. Rev. Lett.* **82**, 1835 (1999).
- [7] A. Sørensen and K. Mølmer, *Phys. Rev. Lett.* **82**, 1971 (1999).
- [8] G. Milburn, S. Schneider, and D. F. V. James, *Fortschritte der Physik* **48**, 801 (2000).
- [9] E. Solano, R. L. de Matos Filho, and N. Zagury, *Phys. Rev. A* **59**, R2539 (1999).
- [10] V. M. Schäfer, C. J. Ballance, K. Thirumalai, L. J. Stephenson, T. G. Ballance, A. M. Steane, and D. M. Lucas, *ArXiv e-prints* (2017), arXiv:1709.06952.
- [11] C. J. Ballance, T. P. Harty, N. M. Linke, M. A. Sepiol, and D. M. Lucas, *Phys. Rev. Lett.* **117**, 060504 (2016).
- [12] J. P. Gaebler, T. R. Tan, Y. Lin, Y. Wan, R. Bowler, A. C. Keith, S. Glancy, K. Coakley, E. Knill, D. Leibfried, and D. J. Wineland, *Phys. Rev. Lett.* **117**, 060505 (2016).
- [13] C. Ospelkaus, U. Warring, Y. Colombe, K. R. Brown, J. M. Amini, D. Leibfried, and D. J. Wineland, *Nature* **476**, 181 (2011).
- [14] T. P. Harty, M. A. Sepiol, D. T. C. Allcock, C. J. Ballance, J. E. Tarlton, and D. M. Lucas, *Phys. Rev. Lett.* **117**, 140501 (2016).
- [15] T. Monz, P. Schindler, J. T. Barreiro, M. Chwalla, D. Nigg, W. A. Coish, M. Harlander, W. Hänsel, M. Hennrich, and R. Blatt, *Phys. Rev. Lett.* **106**, 130506 (2011).
- [16] Shi-Liang Zhu, C. Monroe, and L.-M. Duan, *Europhys. Lett.* **73**, 485 (2006).
- [17] C. F. Roos, *New Journal of Physics* **10**, 013002 (2008).
- [18] S. Debnath, N. M. Linke, C. Figgatt, K. A. Landsman, K. Wright, and C. Monroe, *Nature* **536**, 63 (2016).
- [19] K. Kim, M.-S. Chang, R. Islam, S. Korenblit, L.-M. Duan, and C. Monroe, *Phys. Rev. Lett.* **103**, 120502 (2009).
- [20] T. Choi, S. Debnath, T. A. Manning, C. Figgatt, Z.-X. Gong, L.-M. Duan, and C. Monroe, *Phys. Rev. Lett.* **112**, 190502 (2014).
- [21] T. J. Green and M. J. Biercuk, *Phys. Rev. Lett.* **114**, 120502 (2015).
- [22] C. J. Trout, M. Li, M. Gutierrez, Y. Wu, S.-T. Wang, L. Duan, and K. R. Brown, *ArXiv e-prints* (2017), arXiv:1710.01378.
- [23] Y. Tomita and K. M. Svore, *Phys. Rev. A* **90**, 062320 (2014).
- [24] C. Horsman, A. G. Fowler, S. Devitt, and R. V. Meter, *New Journal of Physics* **14**, 123011 (2012).
- [25] A. M. Stephens, *Phys. Rev. A* **89**, 022321 (2014).